Journal of Materials Chemistry B

PAPER

View Article Online
View Journal | View Issue

Cite this: J. Mater. Chem. B, 2014, 2, 1891

Tailor-made gemcitabine prodrug nanoparticles from well-defined drug–polymer amphiphiles prepared by controlled living radical polymerization for cancer chemotherapy†

Weiwei Wang,[a] Chen Li,[a] Ju Zhang,[a] Anjie Dong[b] and Deling Kong*[a]

Received 5th November 2013
Accepted 14th January 2014

DOI: 10.1039/c3tb21558j

www.rsc.org/MaterialsB

The therapeutic efficacy of gemcitabine is severely compromised by its rapid plasma degradation and low tumor-targeting efficiency. Furthermore, the hydrophilic properties of gemcitabine also make efficient encapsulation and *in vivo* release of the compound difficult in a nanoscale drug delivery system. Herein, gemcitabine–poly(methyl methacrylate) (Gem–PMMA) conjugated amphiphiles were prepared from a gemcitabine-bearing trithiocarbonate initiator *via* reversible addition–fragmentation chain transfer (RAFT) polymerization. The prodrug conjugate with a high drug payload can self-assemble in water into nanoparticles with an average diameter of 130 nm. In addition, gemcitabine molecules within the Gem–PMMA nanoparticles mainly exist in an amorphous state, implicating better gemcitabine release. Indeed, the releasing kinetics of gemcitabine was pH-dependent and a controlled release of gemcitabine from the nanoparticles was observed with 71.6% of cumulative drug release in 72 h in the presence of protease cathepsin B. The cytotoxicity of the gemcitabine prodrug nanoparticles was evident as demonstrated by an *in vitro* viability assay using human pulmonary carcinoma, A549, and breast cancer cells, MCF-7. *In vivo* assessment of the gemcitabine-loaded nanoparticles using BALB/c nude mice with A549 cell derived xenograft tumors indicated that these intravenously administered nanoparticles efficiently inhibit tumor growth as well as alleviate the drug-associated side effects at a dose of 26 mg kg^{-1}. In summary a prodrug nanoparticle, Gem–PMMA, with excellent delivery efficiency and tumor growth inhibition efficacy, was designed and produced. Our results demonstrated the potential of the gemcitabine prodrug nanoparticles as a promising therapeutic formulation for chemotherapy.

1. Introduction

Malignancy is currently the second major cause of global deaths. Increasing research effort has focused on designing drug-loaded polymeric nanoparticles, which may provide effective means for clinical targeting of cancers as well as other diseases.[1–7] These nanoconstructs could be commonly obtained by encapsulation of a certain drug compound during aqueous self-assembly of amphiphilic copolymers, which improves the aqueous solubility of hydrophobic drugs. This approach also stabilizes the chemical activity of medical compounds and enhances the permeability and retention (EPR) effect, resulting in an increased systemic circulation period and drug targeting respectively.[8] However, several limitations of this drug delivery approach have been reported that may hamper the clinical efficacy of chemotherapy. Premature burst release is one of the limiting factors that may cause adverse side effects and danger to patients by rapid release of the encapsulated chemotherapeutic agent before reaching its designated tumor target. Another detrimental factor is the high tendency of poorly soluble drugs to crystallize within the hydrophobic core of nanoparticles during encapsulation, which can inhibit drug release in the targeted tissues. Moreover, the efficiency of maximum drug encapsulation is only a few percent due to the self-interaction of the medical agents as well as interactions between drugs and the hydrophobic core of the nanoparticles. The resulting low delivery efficiency in turn requires a large amount of nanocarriers, which is a common health concern. Lastly, encapsulation of aqueous soluble drugs into nano-sized delivery systems is a highly difficult and complex process. Even though encapsulation has been proved to be successful, a sustainable drug release is usually hard to achieve. Given the limitations of the current nanocarriers, other means to facilitate targeted drug delivery have been investigated. The engineering of prodrugs has been considered as an alternative.[9–18] Promising

[a]Tianjin Key Laboratory of Biomaterial Research, Institute of Biomedical Engineering, Chinese Academy of Medical Science and Peking Union Medical College, Tianjin, 300192, China. E-mail: kongdeling@nankai.edu.cn

[b]School of Chemical Engineering and Technology, Tianjin University, Tianjin, 300072, China

† Electronic supplementary information (ESI) available. See DOI: 10.1039/c3tb21558j

results from clinical trials using macromolecule–drug conjugates (*e.g.*, albumin-bound paclitaxel[19,20]) reported better anti-cancer efficacy, further supporting the suggestion of using other synthetic polymers as delivery vehicles for drug targeting.

Prodrugs are biologically reversible derivatives of intended drug compounds. After administration, they could undergo enzymatic or chemical transformation to release active parent drugs, which could then exert the desired pharmacological effects *in vivo*. In terms of polymeric prodrug synthesis, the commonly used approach is to chemically attach hydrophobic drugs to a prefabricated hydrophilic polymer such as poly(ethylene glycol),[21,22] poly(L-glutamic acid),[13] poly(*N*-2-hydroxypropyl methacrylamide),[23] or dextran[24] to produce fully water-soluble conjugates or small-sized aggregates in an aqueous environment. This strategy has the potential to overcome limitations such as low drug payload, rapid pre-systemic metabolism and toxicity that are commonly observed in the drug delivery system using encapsulative nanocarriers.[25–29] A similar approach has been reported by conjugating pharmaceutical agents to amphiphilic copolymers, which also showed improvements in drug delivery.[2,14,30–32] However, some major issues still remain to be considered, including how to maximize drug loading and precisely regulate the drug payload. Currently, for water-soluble drugs, some efforts have been made to modify their hydrophobic nature to facilitate the encapsulation into another nanoparticle or liposome carrier,[9,33] however, this method inhibits effective drug release, its subsequent diffusion and permeation into targeted tumors.

Herein, a new category of anti-cancer prodrug nanocarriers has been generated with a tailor-made high drug payload and delivery efficiency. These prodrug nanoparticles were assembled from amphiphilic drug–polymer conjugates that are obtained *via* reversible addition–fragmentation chain transfer (RAFT) polymerization, a controlled living radical polymerization technique. In this study, we report a new approach by conjugating the intended drug molecule to a gemcitabine (Gem)-bearing trithiocarbonate initiator, from which a polymer chain composed of a poly(methyl methacrylate) (PMMA) oligomer could be produced in a highly regulated manner. In this way, an amphiphilic drug–polymer conjugate could be generated with the hydrophilic drug molecule at the end of a hydrophobic polymer long chain (Scheme 1). The amphiphilic nature of the drug–polymer conjugates would subsequently propel self-assembly of these prodrug amphiphiles to form nanoscale aggregates in an aqueous environment, by which drug loading and delivery could be achieved. The chemical structure of the drug–polymer conjugate was characterized by ^{1}H NMR and gel permeation chromatography (GPC). Dynamic light scattering (DLS) and transmission electron microscopy (TEM) were employed to assess the physical characteristics and morphology of the drug–polymer nanoparticles in water. The thermodynamic state of the drug molecules was examined using differential scanning calorimetry (DSC) and X-ray diffraction (XRD). The drug releasing profile from the prodrug conjugate and its cytotoxicity were determined by *in vitro* assays using human pulmonary carcinoma A549 and breast cancer cells MCF-7. The efficiency and efficacy of drug delivery of the prodrug were also investigated by *in vivo* analysis following intravenous injection of the prodrug nanoparticles into mice that have developed advanced breast cancer.

2. Materials and experiments

2.1 Materials

Gemcitabine hydrochloride (Gem·HCl), hexylamine, 1-(3-dimethylaminopropyl)-3-ethylcarbodiimide hydrochloride (EDC·HCl) and *N*-hydroxysuccinimide (NHS) were used as received from Sigma-Aldrich. Methyl methacrylate (MMA) from Sigma-Aldrich was distilled under reduced pressure to eliminate the inhibitor prior to use. The RAFT agent precursor *S*-1-dodecyl-*S*′-(α,α′-dimethyl-α″-acetic acid)trithiocarbonate was synthesized according to a previous method.[34] Tetrahydrofuran (THF) and dimethyl sulfoxide (DMSO) were obtained from Jiangtian chemical company and distilled over sodium/benzophenone before use. Dimethyl formamide (DMF) was dried over magnesium sulfate and distilled under reduced pressure just before use.

2.2 Synthesis of Gem-terminated trithiocarbonate

The RAFT agent, Gem-terminated trithiocarbonate was prepared through the amidation of an amino group on a gemcitabine molecule and a carboxyl group on *S*-1-dodecyl-*S*′-(α,α′-dimethyl-α″-acetic acid)trithiocarbonate. The synthesis route is shown in Scheme 1. Generally, Gem·HCl (300 mg, 1 mmol) was firstly dissolved in dry DMF with triethylamine (139 μL, 1 mmol). *S*-1-Dodecyl-*S*′-(α,α′-dimethyl-α″-acetic acid)trithiocarbonate (364 mg, 1 mmol) was also dissolved in dry DMF and activated with EDC/NHS for 2 h. Then the gemcitabine solution was added into the above mixture and the reaction was performed at room temperature for 24 h. The crude products were diluted with ethyl acetate, washed with 10% hydrochloric acid, saturated $NaHCO_3$ and brine, and dried over $MgSO_4$. The solvent was removed under vacuum and the product was further separated by chromatography on silica using 20% petroleum ether in ethyl acetate as eluent. Yield: 347 mg, yellow solid

Scheme 1 The strategy to achieve well-defined polymer–drug conjugate nanoparticles by reversible addition–fragmentation chain transfer (RAFT) polymerization.

(0.569 mmol, 52.3%). ^{1}H NMR (DMSO-d_6, 500 MHz): δ 10.27 (s, 1H, CONH), 8.03 (d, 1H, H-a′), 7.47 (d, 1H, H-b′), 6.21 (d, 1H, H-c′), 5.83 (s, 1H, H-d′), 5.30 (t, 1H, H-e′), 4.30 (m, 4H, H-f′–h′), 3.28 (m, 2H, –SCS_2CH_2–), 1.60 (m, 4H, –$NHCOC(CH_3)_2$–), 1.22 (m, 20H, –$SCS_2CH_2(CH_2)_{10}CH_3$), 0.84 (s, 3H, –$SCS_2CH_2(CH_2)_{10}CH_3$).

2.3 Synthesis of Gem–PMMA conjugates

RAFT polymerization was employed to prepare Gem–PMMA prodrug conjugates. A typical procedure was as follows: MMA (600 mg, 6 mmol), Gem-RAFT (305 mg, 0.5 mmol) and 2,2′-azodiisobutyronitrile (8.2 mg, 0.05 mmol) were dissolved in 2 mL of dimethyl sulfoxide. The mixture was degassed by three cycles of freeze–pump–thaw and sealed with argon. After stirring at 60 °C for 12 h, the crude product was precipitated in excess diethyl ether to give the precursor Gem–PMMA as a light yellow powder. Then Gem–PMMA (173 mg, 0.1 mmol) was redissolved in dimethyl sulfoxide (2 mL), and hexylamine (51 mg, 0.5 mmol) was added to the solution. The reaction mixture was stirred for 1 h at room temperature under a nitrogen atmosphere. After precipitation in diethyl ether, filtration and drying under vacuum, the final Gem–PMMA was harvested as a colorless powder. The polymerization degree of MMA and the aminolysis of the thiocarbonylthio groups were confirmed by ^{1}H NMR (Varian INOVA 500 MHZ, solvent: DMSO-d_6) and gel permeation chromatography (GPC, Viscotek GPCmax, Malvern).

2.4 Characterization of gemcitabine in Gem–PMMA

The physical state of gemcitabine in Gem–PMMA conjugates was investigated using DSC (NETSCZ 204, Germany) and XRD (Bruker D8-S4, Germany). Gem–PMMA powders were subjected to DSC and XRD analyses with native gemcitabine as the control. For DSC measurement the heating rate was 10 °C min^{-1} in the temperature range of 30–200 °C, whereas for X-ray diffraction the diffraction angle 2θ was recorded from 6° to 60° with a scanning speed of 10° min^{-1} and copper was used as the source of X-ray radiation at 40 kV with 40 mA.

2.5 Self-assembly and characterization of Gem–PMMA conjugates in water

Due to the amphiphilic nature of Gem–PMMA, the self-assembly of nanoparticles was prepared using the nanoprecipitation technology. Typically, twenty milligrams of Gem–PMMA were dissolved in 4 mL of dimethyl sulfoxide and the resulting solution was slowly added dropwise into 20 mL of ultrapure water. Dimethyl sulfoxide was removed by dialysis. The final Gem–PMMA concentration was adjusted to 1 mg mL^{-1}.

The hydrodynamic size of Gem–PMMA nanoparticles in water was studied using a dynamic light scattering (DLS) instrument (Brookhaven BI-200SM, USA) at λ = 532 nm under room temperature. Measurements of scattered light were fixed at an angle of 90° to the incident beam. The results of DLS were analyzed by the regularized CONTIN method. The zeta potential of Gem–PMMA particles in water was determined using a Malvern Zetasizer Nano ZS (Malvern Instruments Ltd, MA). The morphology and core size of Gem–PMMA nanoparticles were determined by using a JEM-2100F transmission electron microscope at an accelerating voltage of 200 kV.

2.6 *In vitro* drug release

In vitro release of gemcitabine from polymer–drug conjugate nanoparticles was investigated with or without the presence of protease cathepsin B (5 U mL^{-1}). Gem–PMMA conjugates were formulated in acetate buffer (20 mL, pH 5.0) containing 400 μL of enzyme or PBS buffer (20 mL, pH 6.8 or 7.4). Samples in dialysis tubes were prepared in triplicate and shaken at 100 rpm at 37 °C. At regular time intervals, samples (3 mL) were withdrawn and the content of free or conjugated gemcitabine was analyzed from the UV spectrum. Then the cumulative release of gemcitabine was calculated.

2.7 Cell culture

The human lung carcinoma cell line (A549) was obtained from Sigma-Aldrich and the human breast adenocarcinoma cell line (MCF-7) was kindly provided by Professor Anli Jiang from the Institute of Biochemistry and Molecular Biology, Medical School of Shandong University. A549 cells were maintained in Hyclone Ham's/F12 medium. MCF-7 cells were cultured in Hyclone DMEM/high glucose medium. All media were supplemented with 10% heat-inactivated fetal bovine serum (FBS), penicillin (100 U mL^{-1}) and streptomycin (100 μg mL^{-1}). All cell lines were maintained at 37 °C and 5% CO_2 in a humidified atmosphere.

2.8 *In vitro* and *in vivo* anti-tumor activity of gemcitabine

The *in vitro* cytotoxicity of free gemcitabine or Gem–PMMA conjugate nanoparticles was evaluated on the above two cell lines by the cell counting kit-8 (CCK-8) viability test. Briefly, cells were seeded in 100 μL of culture medium (5×10^3 cells per well) in 96-well microtiter plates and pre-incubated for 24 h. The cells were then exposed to a series of gemcitabine or Gem–PMMA solutions of different concentrations for 48 h. After incubation, 10 μL of CCK-8 (Dojindo, Japan) solution in phosphate-buffered saline was added to each well. After incubation for 60 min, the absorbance of the solubilized dye was measured spectrophotometrically with a microplate reader (Thermo Scientific Varioskan Flash) at 450 nm. The percentage of viable cells in each well was calculated as the absorbance ratio between treated and untreated control cells. All experiments were set up in quintuplicate to determine mean values and standard deviations (SDs).

In vivo anti-tumor activity was evaluated using xenograft tumor models. All animal experiments were performed in accordance with the protocol approved by the Tianjin Institute of Medical and Pharmaceutical Science. Xenograft tumors were subcutaneously implanted in 6–7 weeks old male BALB/c nude mice (Vital River Laboratory Animal Technology Co. Ltd, China) by the injection of 200 μL of A549 cell (2×10^6) suspension in the upper portion of the right flank. The treatment was initiated when the tumor reached approximately 100–150 mm^3. The mice were randomly assigned to one of the three treatment groups. Group 1 (n = 10), mice were untreated as the control group; group 2 (n = 10), mice received intravenous injection of

gemcitabine (26 mg kg^{-1}); group 3 ($n = 10$), mice received intravenous administration of Gem–PMMA (26 mg kg^{-1}). The tumor volumes were measured using a caliper and calculated according to the formula, tumor volume $= a^2 \times b/2$, where a is the shorter diameter and b is the longer one. The body weight of the animals was also recorded every two days. The statistical difference was analyzed by the one-way ANOVA method and the results were expressed as mean ± SD. $p < 0.05$ was considered as significant.

3. Results

3.1 Synthesis and characterization of gemcitabine–poly(methyl methacrylate) (Gem–PMMA) conjugates

Gemcitabine is a nucleoside analogue, which acts against a wide range of solid tumors, including pancreatic, non-small lung, breast, and ovarian.[10,35,36] Clinical trials using gemcitabine for melanoma therapy have also been reported.[37] Despite its effective anti-cancer activity, gemcitabine suffers from various drawbacks, such as rapid deamination to inactive 2′,2′-difluorodeoxyuridine by cytidine deaminase after intravenous injection, resulting in a short *in vivo* half-life (8–17 min).[9] Furthermore, a lower level of transportation of gemcitabine into cells, resulting from blocked uptake due to decreased expression of different transporters, such as hENT1, also restricts its anti-cancer activity.[35] Therefore, a strategy that both provides protection of the amino group on the 4-(*N*)-site and enhanced transport by chemical modification of the gemcitabine molecule could potentially lead to novel therapeutic formulations. Inspired by this, the preparation of gemcitabine prodrug nanoparticles was proposed and the RAFT technique, which offers incomparable flexibility in the construction of advanced macromolecular architectures, was performed to prepare the gemcitabine–poly(methyl methacrylate) (Gem–PMMA) conjugate macromolecules. The synthesis route is depicted in Fig. 1. The gemcitabine end functionalized poly(methyl methacrylate) was synthesized from the polymerization of methyl methacrylate (MMA) under traditional radical initiation in the presence of the Gem-based trithiocarbonate RAFT agent. As an initial step, the trithiocarbonate RAFT moiety *S*-1-dodecyl-*S*′-(α,α′-dimethyl-α″-acetic acid) was synthesized. Then gemcitabine was chemically conjugated to it through the amidation of the 4-(*N*)-site amino group of gemcitabine and the carboxyl group of the trithiocarbonate moiety using EDC/NHS coupling chemistry. As the amino group is more prone to react with the carboxyl group compared to the hydroxyl group, the selectivity and yield of the conjugation procedure were acceptable.

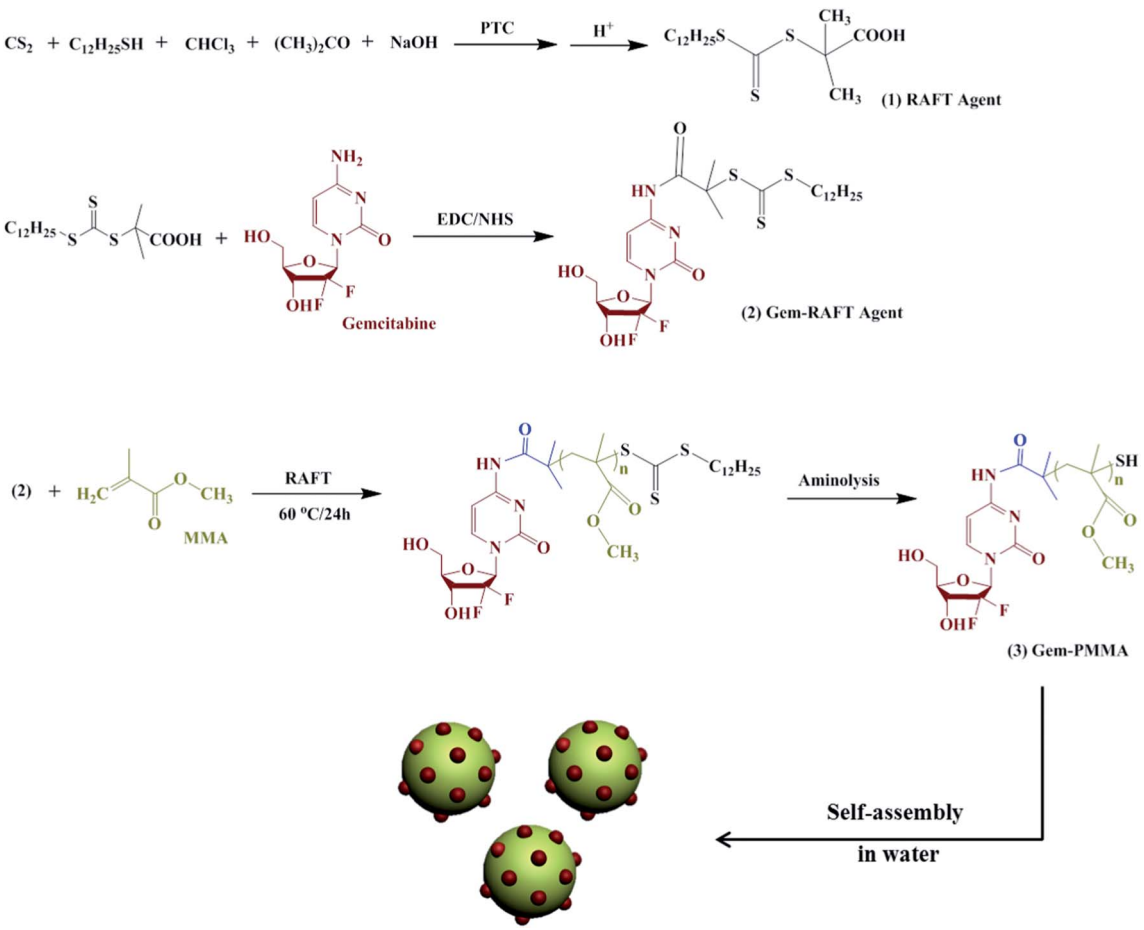

Fig. 1 The design of Gem–PMMA conjugate nanoparticles.

Table 1 Characterization of gemcitabine–poly(methyl methacrylate) (Gem–PMMA) conjugates and nanoparticles

Gem–PMMA	M_n[a] (g mol^{-1})	PDI[b]	Size[c] (nm)	PDI[c]	ξ[d] (mV)	%Gem[e] (wt%)
Gem–PMMA5	865	1.23	123 ± 3	0.13	−65.3	43.7
Gem–PMMA11.2	1485	1.21	136 ± 4	0.14	−64.9	21.5

[a] Determined by ^{1}H-NMR. [b] Detected by GPC. [c] Determined by DLS. [d] Zeta potential determined using a Zetasizer (Malvern). [e] %Gem = M_n(Gem)/M_n(PMMA).

The RAFT polymerization of MMA was carried out in anhydrous DMSO at 60 °C under azodiisobutyronitrile radical initiation and Gem–PMMA with low dispersity and controlled hydrophobic segment length was obtained. By varying the feeding amount of MMA monomers, two representative Gem–PMMAs with a tailor-made and high drug payload were constructed as shown in Table 1. The chemical structure of Gem–PMMA was firstly confirmed by ^{1}H NMR (Fig. 2). The characteristic proton peaks in the chemical shift range of 4.0–9.0 ppm attributed to Gem, proton peaks at δ = 3.55 ppm ascribed to the methyl of PMMA and that at δ = 1.21 ppm assigned to methylene groups of the initiator all appear in the ^{1}H NMR spectra, which confirm the successful polymerization of MMA. In order to eliminate the potential biological toxicity of trithiocarbonates and obtain a functional living thiol group, a subsequent aminolysis was performed to break the thiocarbonylthio group. The disappearance of proton peaks at δ 0.83, 1.21 and 3.20 ppm assigned to methylene and methyl of dodecyl demonstrated the complete fragmentation of the thiocarbonylthio moiety. The molecular weight of hydrophobic PMMA in Gem–PMMA calculated from ^{1}H NMR was 500 and 1120, respectively. Thus, the corresponding gemcitabine weight fractions in Gem–PMMA conjugates were 43.7 and 21.5 wt%, respectively. Furthermore, the molecular weight distribution detected by GPC was approximately 1.2. An advantage of the synthetic strategy of growing MMA from the Gem-based RAFT agent is that the weight fraction of gemcitabine in the resulting conjugate can be fine-tuned by adjusting the hydrophobic polymer chain length through altering the initial stoichiometry of the monomers. Significantly, the drug payload could be easily increased to over 20 wt% by reducing the polymer chain length, which is certainly owed to the controlled living radical polymerization technique implemented here.

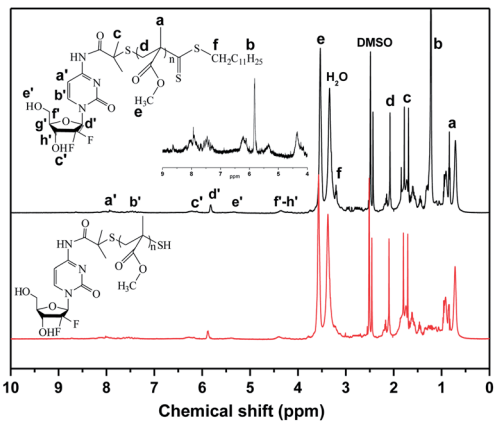

Fig. 2 The ^{1}H NMR spectra of Gem–PMMA conjugates.

The chemical conjugation of gemcitabine was further determined by UV-vis spectroscopy. As depicted in Fig. S1 (ESI†), the maximum absorption peak of native gemcitabine appeared at a wavelength of 268 nm, however, that of gemcitabine in Gem–PMMA conjugates was around 305 nm. This red shift of wavelength indicated that gemcitabine was chemically linked to PMMA by an amide bond, which has a stronger electronegativity compared to the amino group.[38–40] The prominent difference in ultraviolet absorption of free or conjugated gemcitabine was then utilized to characterize the hydrolysis of Gem–PMMA under the catalysis of cathepsin.

3.2 Characterization of gemcitabine in Gem–PMMA

The physical state of a drug in nanoparticles or other formulations can influence the drug loading capacity, the homogeneity of the drug in the formulation, the stability of the formulation as well as the therapeutic effect.[41,42] Generally, drugs encapsulated in the hydrophobic core of nanoparticles with a high drug payload tend to crystallize, which could inhibit the effective and complete release of the drug.[34] Conversely, increasing the amorphous fraction of the drug can improve the sustained release of the drug. Therefore, the state of gemcitabine in Gem–PMMA conjugates was analyzed by DSC and XRD. As can be seen from Fig. 3A, the melting endotherm of pure gemcitabine appeared at 168 °C, nevertheless, no obvious melting peak of gemcitabine was detected for Gem–PMMA conjugates even with a drug payload as high as 43.7 wt%. It can thus be concluded that gemcitabine in Gem–PMMA was in an amorphous state. The information obtained from XRD (Fig. 3B) complied with the results obtained from DSC analysis. The disappearance of the characteristic crystalline peak of gemcitabine suggested that gemcitabine in Gem–PMMA was in the amorphous state, which would avoid the above-mentioned undesirable outcomes resulting from drug crystallization.

3.3 Formation and characterization of Gem–PMMA nanoparticles in water

Due to the amphiphilic nature of the macromolecular conjugates, the nanoprecipitation technique was performed without any additional stabilizer to prepare Gem–PMMA nanoparticles by self-assembly of Gem–PMMA conjugates in aqueous solution. The hydrodynamic size and morphology of obtained nanoparticles were characterized by DLS and TEM (Fig. 4). The average diameters of Gem–PMMA5 and Gem–PMMA11.2 nanoparticles were 123 nm and 136 nm, respectively, which are suitable for

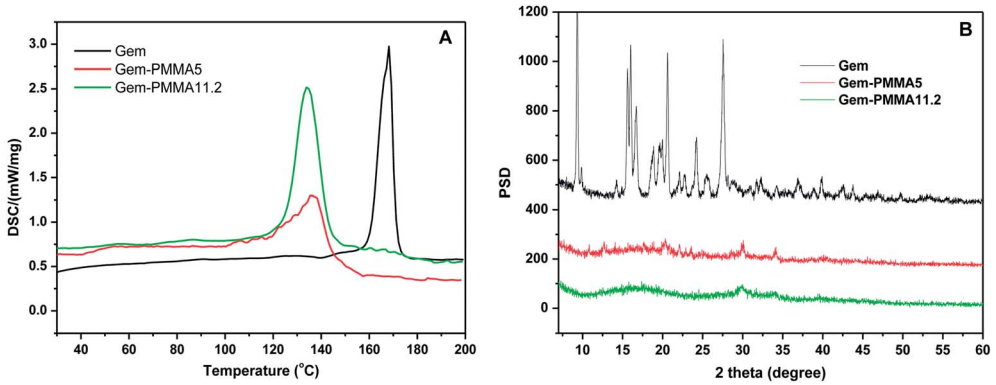

Fig. 3 The DSC and XRD curves of gemcitabine and Gem–PMMA conjugates.

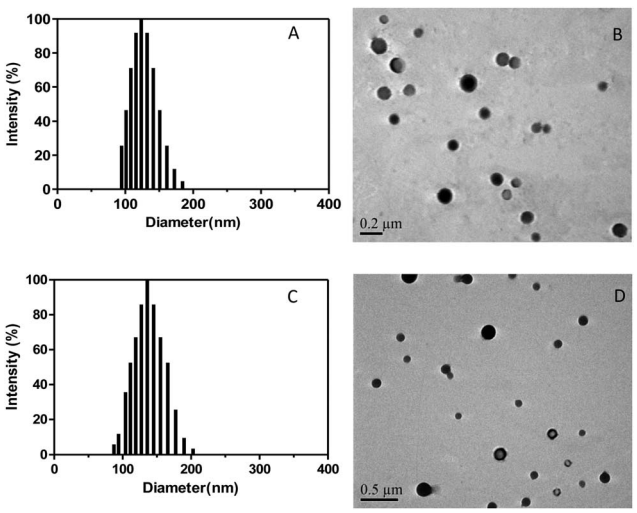

Fig. 4 The diameter and TEM images of Gem–PMMA5 (A and B) and Gem–PMMA11.2 (C and D) prodrug nanoparticles.

intravenous administration. The zeta potential of conjugate polymers was around −65 mV. No clear dependence of the nanoparticle size and the surface zeta potential on the polymer chain length was observed. The distribution indices of both nanoparticles were all below 0.15 as determined by DLS, indicating a monodisperse system. Prodrug nanoparticles were further characterized by TEM and the images showed that Gem–PMMA nanoparticles had spherical morphologies. Interestingly, a small part of Gem–PMMA conjugates likely assembled into vesicles due to the high ratio of molecular weight of PMMA in Gem–PMMA conjugates. Significantly, another water-insoluble anticancer drug can be simultaneously incorporated into the core of prodrug nanoparticles *via* hydrophobic interactions without any unfavorable influence on the pre-conjugated gemcitabine, which can be considered as a potent strategy in combination chemotherapy. Furthermore, the obtained thiol at the extremity of the prodrug amphiphile can be utilized as an active target to conjugate a target molecule such as a polypeptide, or conjugate the prodrug amphiphile to other particles, for example, golden nanoparticles, quantum dots through the thiol–ethylene reaction or a disulfide linkage to produce a versatile nano-platform.

3.4 *In vitro* gemcitabine release

In vitro gemcitabine release studies were carried out under different pH environments (7.4, 6.8, and 5.5) to mimic the blood circulation environment, the extracellular matrix of tumor tissue and the lysosomal compartment within a cancer cell. The amide bond, which is often designed for enhanced oral absorption by synthesizing substrates of specific intestinal uptake transporters,[43] was used to link the gemcitabine molecules and the PMMA segment. An amide bond is usually hydrolyzed by ubiquitous carboxyl esterases, peptidases or proteases.[9,44] And it has been proven that substituents in the α-position of amide, such as methyl or vinyl can greatly accelerate the hydrolysis of amide at an acidic pH.[45] Thus, the hydrolysis of amide was investigated to deduce the gemcitabine release in the presence or absence of lysosomal proteolytic enzyme cathepsin B. The hydrolysis of amide was monitored by UV-vis spectroscopy. As shown in Fig. 5A, the intensity of absorbance at 268 nm assigned to free gemcitabine gradually increased while that of Gem–PMMA decreased as the hydrolysis time increased, demonstrating the occurrence of amide breakage. Fig. 5B reveals that Gem–PMMA prodrug nanoparticles can sustain and control the release of gemcitabine and the hydrolysis of methyl substituted amide was pH-dependent. After hydrolysis for 72 h at pH 5.5, approximately 46.8% of initial gemcitabine was released. The presence of cathepsin B obviously accelerated the hydrolysis of gemcitabine from the Gem–PMMA conjugate and after 72 h, so the cumulative release of gemcitabine was about 71.6%. However, at pH = 7.4 only 10% of total conjugated gemcitabine was liberated, indicating that Gem–PMMA conjugate prodrug nanoparticles could effectively inhibit the burst release and subsequently decrease the deamination by cytidine deaminase in plasma. Additionally, it seemed that the poor degradability of the hydrophobic block did not influence the gemcitabine release kinetics, which has also been observed in the poly(L-glutamic acid)–paclitaxel conjugate.[46]

3.5 *In vitro* cytotoxicity assay

The cytotoxic activity of gemcitabine was evaluated by incubating A549 and MCF-7 cells with free gemcitabine or

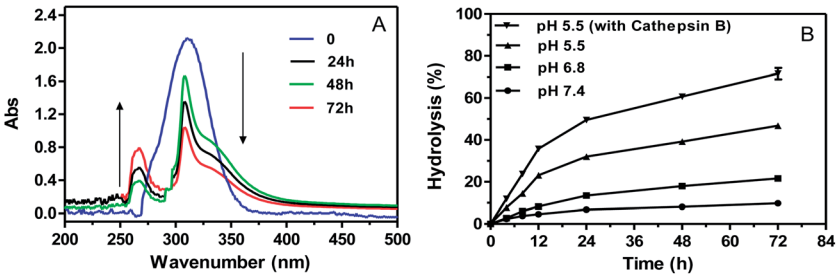

Fig. 5 The UV-vis (A) monitoring of the hydrolysis of Gem–PMMA conjugates and the cumulative release (B) of gemcitabine calculated from the hydrolysis.

gemcitabine conjugated prodrug nanoparticles for 72 h and the cell viability was determined using the CCK-8 assay. It has been well recognized that poly(methyl methacrylate) based nanoparticles show no cytotoxicity to various cancer cells.[47–49] Nevertheless, in this study the cytotoxicity of the PMMA derivative, prepared by RAFT polymerization *via* the non-gemcitabine modified RAFT agent and followed by aminolysis, was implemented. The result (Fig. 6C) indicated that the PMMA derivative was not toxic to A549 and MCF-7 cells with a cell variability of above 90% compared to the control group The formulation of Gem–PMMA nanoparticles was found to be cytotoxic to both A549 and MCF-7 cells and the cell viability was decreased as the concentration of gemcitabine increased (Fig. 6). Both formulations can cause a median lethal when the dose was increased to approximately 2 μM. Although it was a prodrug, Gem–PMMA nanoparticles and free gemcitabine exhibited comparable cytotoxicity without any statistical significance. This was possible as it has been proven that drug-loaded nanoparticles were prone to be endocytosed through cell membrane-mediated fusion.[14,50,51] In addition, deducing from the *in vitro* release, intracellular Gem–PMMA nanoparticles could persistently and effectively release gemcitabine molecules under the stimulation of an acidic environment and the catalysis of cathepsin. All these behaviors render the Gem–PMMA prodrug nanoparticles cytotoxic against A549 and MCF-7 cells.

3.6 *In vivo* anti-tumor activity

The *in vivo* anti-cancer activity of gemcitabine conjugated prodrug nanoparticles was tested in an A549 cell derived xenograft model in BALB/c nude mice. The intravenous injection of gemcitabine or Gem–PMMA nanoparticles at a dose of 26 mg kg^{-1} was carried out on days 5, 8, 11 after tumor inoculation. Fig. 7A shows that untreated mice (saline 0.9%) exhibited a

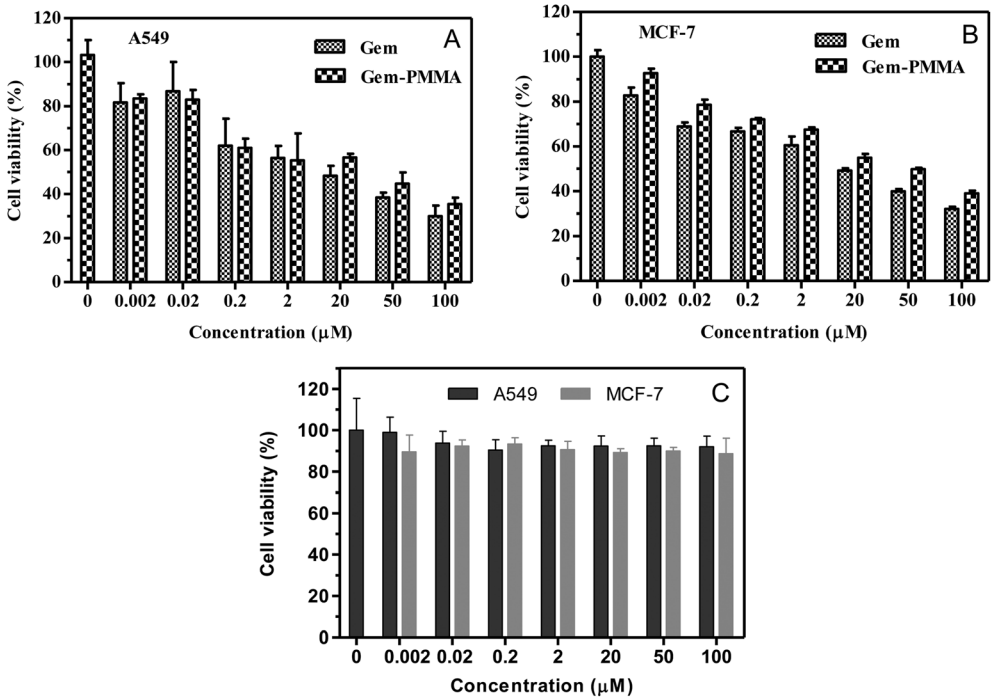

Fig. 6 The *in vitro* cytotoxicity of gemcitabine and Gem–PMMA nanoparticles to A549 (A) and MCF-7 (B) cells and the *in vitro* cytotoxicity of the corresponding PMMA derivative to these cells (C).

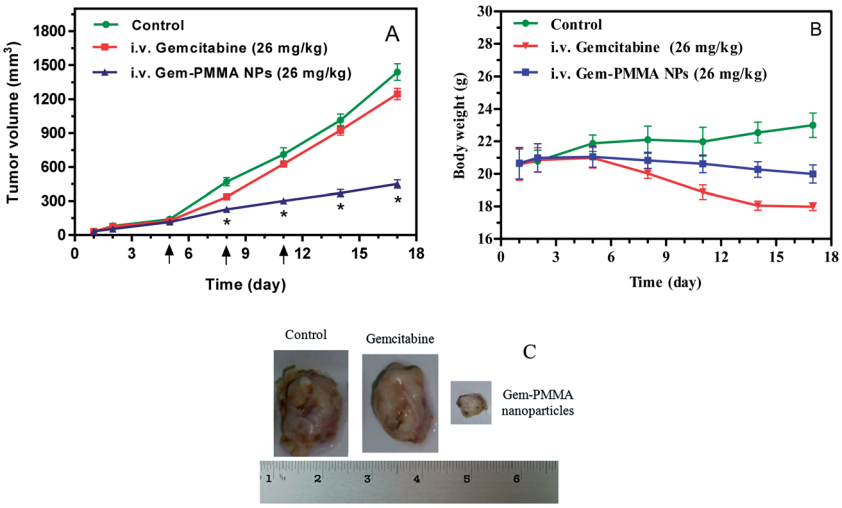

Fig. 7 *In vivo* anti-tumor effect (A) of Gem–PMMA nanoparticles against A549-induced BALB/c nude mice, body weights of the animals (B) and representative tumor tissues for different treatment groups (C). i.v. is the short form for intravenous injection and the arrows indicate the injection schedule. A statistical significance was observed (*$p < 0.05$) after the first injection.

rapid tumor growth, with an average tumor volume of approximately 1441 mm^3 at day 17. Mice treated with gemcitabine showed a similar pattern, with equivalent tumor volumes at the end of the treatment, thus demonstrating the absence of anti-cancer activity of gemcitabine in this model. In contrast, treatment of mice with Gem–PMMA prodrug nanoparticles at the equivalent dose of gemcitabine significantly reduced the tumor growth with inhibition as high as 68%. Statistical significance (p-value of 0.0157) was observed with Gem–PMMA nanoparticle treatment against the control group or Gem treatment. The change in the body weight of the animals was also monitored throughout the treatment (Fig. 7B). Obviously, gemcitabine-treated mice exhibited significant weight loss (approximately 13.3%) compared to that of the control group and this result highlighted the toxicity of the free drug treatment. However, the Gem–PMMA nanoparticle-treated mice exhibited only a slight decrease of body weight (approximately 3.7%). These findings indicated the efficient anti-cancer activity of gemcitabine conjugate prodrug nanoparticles and the effective alleviation of gemcitabine-related adverse effects.

4. Discussions

Gemcitabine is a chemotherapeutic agent that was approved by the FDA in 1996 as the first-line treatment for patients who have been diagnosed with locally advanced (non-resectable Stage II or Stage III) or metastatic (Stage IV) non-small cell lung cancer.[35,52] However, since gemcitabine is rapidly deaminated in the circulation system into its inactive metabolite 2′,2′-difluorodeoxyuridin, it has a short half-life, which requires high dosage (1000 mg m^{-2}) administration to improve its clinical therapeutic index, although adverse side effects are often a health concern. Moreover, tumor resistance against gemcitabine also occurs due to the loss of nucleoside transporters and phosphorylation kinases that are essential for drug entry and activation within the malignant cells.

The use of the prodrug has emerged as a promising drug delivery method that could potentially improve the metabolic stability of chemotherapeutic compounds, enhance their anti-tumor activities and ameliorate chemotherapy-related resistance. For targeted delivery of gemcitabine, various pharmaceutical approaches have focused on chemical modifications of the amino group at the 4-(*N*)-position or the hydroxyl group at the 5′-position of the gemcitabine molecule.[35] These modifications could facilitate conjugation of the drug compound with lipophilic molecules or polymeric carriers, which protect gemcitabine from plasma metabolism. Passive delivery of the drug conjugates into tumor cells is also made possible due to the lipophilic properties of the conjugated polymers. Thus, several lipophilic gemcitabine conjugates including PEG–gemcitabine,[22] squalenoyl–gemcitabine,[53] gemcitabine–polyisoprene[12] and poly(ethylene glycol)-*block*-poly(2-methyl-2-carboxyl-propylene-carbonate)–gemcitabine[9] have all been investigated as potential prodrugs to improve the clinical outcome of gemcitabine chemotherapy. However, several limiting factors of these delivery systems have also been reported which were caused by poor aqueous solubility, low intracellular uptake, nonspecific tumor-targeting, slow drug release or low gemcitabine payload of the gemcitabine conjugates. Moreover, the lack of chemically active groups of the conjugated polymers may also limit further modifications of the gemcitabine conjugates with tumor-targeting molecules, bioactive polypeptides or proteins.

Another approach was using nanoparticles to encapsulate the lipophilic gemcitabine conjugates for better anti-cancer effects. Previous studies have incorporated 4-(*N*)-stearoyl gemcitabine into a nanoparticle made up of a PEGylated stearic acid derivative for lysosomal delivery of gemcitabine.[33] Application of this delivery system successfully prolonged the circulation time of the drug compound in comparison to native gemcitabine. Increased accumulation of gemcitabine was also observed in tumor cells, although an inadequate drug payload (5%) and *in vivo* anti-tumor activity still need to be addressed.

In the present study, a self-assembled amphiphilic gemcitabine–PMMA conjugate was synthesized *via* reversible addition–fragmentation chain transfer (RAFT) polymerization, a process that enables controlled elongation of PMMA oligomers from a gemcitabine (Gem)-bearing trithiocarbonate initiator. The content of gemcitabine within the Gem–PMMA conjugates could be accurately regulated by changing the initial stoichiometry of the MMA monomers. As a result, each of the obtained amphiphiles contains a hydrophobic PMMA backbone and a hydrophilic gemcitabine tail. When dissolved in water, the Gem–PMMA conjugates undergo self-assembly to form nanoparticles with diameters ranging from 120 to 140 nm, which in comparison to PEG–Gem or other low molecular weight Gem-conjugates could increase the metabolic stability, systemic release and intracellular uptake of gemcitabine.

For anti-cancer formulations, accurate preparation of a drug payload is crucial to the performance of chemotherapy. A dynamic drug payload that could be easily adjusted according to tumors of different types, developmental stages and patient compliances would facilitate the efficacy of chemotherapy. Our results showed that the proportion of gemcitabine loading in the Gem–PMMA conjugates was more than 40 w/w%, which is considerably higher than the Gem–PEGylated amphiphilic copolymer micelles, showing a maximum payload of only 12.8 w/w%.[9] More importantly, the gemcitabine payload in our Gem–PMMA nanoparticle formulations could be accurately controlled by regulation of the molecular weight of the PMMA chain during RAFT polymerization. This on-demand regulation of the gemcitabine payload is particularly significant for personalized anti-cancer treatment. Another issue is that during encapsulation, water-insoluble drugs with a high drug payload tend to crystallize within the hydrophobic core of nanoparticles or other formulations, which leads to impaired drug release and consequently inhibited efficacy of chemotherapy.[42] However, our Gem–PMMA carriers do not cause such a problem since the majority of the gemcitabine molecules remained in the amorphous state, as illustrated by DSC and XRD.

Since gemcitabine conjugated prodrug nanoparticles are intended for intravenous administration, it is important that the Gem-containing formulations do not release active gemcitabine during plasma delivery. Premature drug release can cause plasma metabolism of gemcitabine, which in turn leads to low drug concentration and lack of efficacy of gemcitabine at the targeted tissue. Furthermore, after delivery of prodrug nanoparticles to the targeted tumors, drug internalization by lysosomes and endosomes of the tumor cells is required since lysosomes and endosomes provide an acidic and enzyme-rich environment for gemcitabine release. In order to assess the release of free gemcitabine from our Gem–PMMA nanocarriers, drug dissociation from the polymer conjugates was measured in the presence or absence of cathepsin B (a cysteine protease) in an acidic lysosomal environment (pH 5.5), where a pH-depended gemcitabine releasing profile was observed. However, in a neutral environment, only 10% of gemcitabine was dissociated from the conjugates, which increased to 46% when the pH value decreased to 5.5. The accumulative release of gemcitabine further elevated to 70% in the presence of cathepsin B, indicating that the gemcitabine release was dependent not only on acidic hydrolysis between the gemcitabine molecules and PMMA segments, the enzymatic activity of cathepsin B is also important. Cathepsin B is a well recognized lysosomal protease that cleaves the amide bonds between the Gem–PMMA conjugates to release gemcitabine. Previous studies have already reported a significant role of cathepsin to degrade amide bonds in order to release gemcitabine from polymeric conjugates.[8] However, cathepsin B can only function once the Gem-conjugated amphiphilic copolymers are dissociated from their corresponding micelles, which is a time consuming process since the dissociation of micelles is a dynamic equilibrium with the molecularly dissolved copolymer molecules in aqueous solution. As a result, the release of gemcitabine from the hydrophobic cores of amphiphilic copolymer nanoparticles may be delayed. Indeed, a slow releasing profile was observed from PEG–PCC–gemcitabine conjugate micelles, with an accumulative release of only 60% after 10 days,[8] which may be accountable for its inefficient anti-tumor activity. In contrast, for our Gem–PMMA conjugates, gemcitabine acted as a hydrophilic head of Gem–PMMA. In the aqueous environment, these gemcitabine heads are completely exposed to the acidic microenvironment and the Gem–PMMA conjugates can be directly affected by cathepsin B without requirement of predissociation, resulting in a much more rapid releasing process of gemcitabine. Furthermore, although degradation of the PMMA backbone is difficult, PMMA has been proven to be physiologically nontoxic and small polymer chains of PMMA can be effectively excreted.[47–49] Thus, given the challenging task of *in vivo* delivery of water-soluble cancer drugs, our Gem–PMMA conjugates have proven to be a facile method to deliver and release active gemcitabine in a controlled and sustained manner.

To evaluate the efficacy of this Gem–PMMA prodrug nanoparticle delivery system, the anti-tumor activity of gemcitabine was examined both *in vitro* and *in vivo*. It is well known that tumor cell endocytosis is primarily determined by nanoparticle size and surface charge,[54] which were unaffected by the lengths of the PMMA chain within the Gem–PMMA prodrug nanoparticles. Thus, Gem–PMMA5 was used as a representative in the CCK-8 cytotoxicity assay, which demonstrated uncompromised cytotoxic activity of gemcitabine after bioconjugation with the hydrophobic segment (Fig. 6). Moreover, the dose-dependent cytotoxicity of gemcitabine was also observed. However, lower cell viability was observed from free gemcitabine administered A549 and MCF-7 cells in comparison to the Gem–PMMA treated groups, which was mainly due to a relatively slower cell uptake process of the Gem–PMMA nanoparticle *via* endocytosis. The releasing process of gemcitabine from Gem–PMMA may also be attributed to the reduced cytotoxicity of the prodrug nanoparticles since intracellular dissociation of gemcitabine is required before its anti-cancer activity could take effect. Despite the observed *in vitro* cytotoxicity of the free gemcitabine, cell culture studies are inadequate to assess the potential of the Gem–PMMA in chemotherapy. Indeed, in cell culture studies, the free drug molecules directly come into contact with the cancer cells, whereas tumor-targeting,

protection of active gemcitabine from systemic enzyme degradation, mechanisms of drug uptake and its enhanced permeability and retention (EPR) effect are impossible to study *in vitro* due to the lack of physiological interference that commonly occurs during clinical drug administration. Hence, the anticancer activity of free gemcitabine and the Gem–PMMA prodrug nanoparticles was further evaluated using a xenograft mouse model with lung carcinoma. A moderate gemcitabine dosage of 26 mg kg^{-1} was selected based on previous reports.[9,12] Gemcitabine or prodrug nanoparticle formulations were administered *via* tail vain injection using BALB/c nude mice. Following administration of the same amount of gemcitabine/Gem–PMMA, better suppression of tumor growth was observed from the prodrug nanoparticle-treated groups with ameliorated gemcitabine-associated side effects. The higher efficacy of antitumor activity may be resulted from the decreased plasma metabolism of gemcitabine within the Gem–PMMA conjugate since the prodrug nanoparticle could protect gemcitabine from cytidine deaminase-dependent deamination. Enhanced permeation and retention were also evident following Gem–PMMA application due to the nano-sized dimension of the prodrug nanoparticles. Thus, the Gem–PMMA prodrug nanoparticles exhibited comparatively better anti-tumor activity over the free drug treatment groups. Furthermore, the anti-tumor efficacy of the Gem–PMMA was also better than that of the prodrug micelles composed of the gemcitabine–PEGylated amphiphilic copolymer conjugate.[9] In addition to the comparative anti-tumor efficacy compared to previous work by Harrison *et al.*,[12] the slight decrease in body weight of experiment animals treated with prodrug nanoparticles could be attributed to the enhanced dose and more particularly to the different types of cancer and mice, which perhaps affected the pharmacokinetic properties of the drug. Optimizing the dosing schedule may be an effective option to improve the pharmacokinetic–pharmacodynamic profile of gemcitabine prodrug formulation and minimize gemcitabine-associated adverse side effects. Moreover, no significant difference could be detected between the control group and the free gemcitabine administered group, consistent with previous studies.[9,10,22,33] The lack of the anti-tumor effect in the free gemcitabine-treated animals may be due to the rapid plasma degradation of free gemcitabine, which in turn results in an inadequate level of gemcitabine at the tumor site.

Taken together, the gemcitabine payload of the Gem–PMMA prodrug nanoparticles could be tailor-made and enhanced *via* controlled living radical polymerization. The obtained gemcitabine conjugated prodrug nanoparticles were able to protect gemcitabine from rapid plasma metabolism *in vivo*. A controlled and sustained gemcitabine release profile was also evident, implicating the potential of the Gem–PMMA in gemcitabine delivery. *In vivo* analysis using BALB/c nude mice with lung cancer exhibited the enhanced anti-tumor activity of gemcitabine and reduced drug-associated side effects from the Gem–PMMA treated group, indicating that the drug conjugated PMMA prodrug nanoparticles may be promising candidates for efficient delivery of water-soluble anti-cancer drugs.

5. Conclusion

We report here a new strategy for gemcitabine–polymer prodrug conjugate preparation, which is dependent on the controlled elongation of poly(methyl methacrylate) (PMMA) by RAFT polymerization from a gemcitabine-functionalized trithiocarbonate initiator. The obtained prodrug conjugates could then self-assemble in water into narrowly dispersed nanoparticles with diameters in the range of 120–140 nm. The drug payload could also be tailor-made by accurately adjusting the molecular weight of the PMMA oligomer, resulting in a drug payload of more than 40 w/w%. In addition, instead of drug crystallization within the hydrophobic core of the nanocarriers, gemcitabine remained in the amorphous state and its release from conjugate nanoparticles was pH-dependent. Gemcitabine release could also be enhanced in the presence of Cathepsin B. Results from *in vitro* cytotoxicity assays demonstrated the efficient anticancer activity of the Gem–PMMA prodrug nanoparticles in human pulmonary carcinoma A549 and breast cancer MCF-7 cells. The Gem–PMMA prodrug nanoparticles also exhibited more efficient tumor suppression effects compared to free gemcitabine-treated mice with ameliorated gemcitabine-associated side effects. In summary, our results implicated the potential of the gemcitabine prodrug nanoparticles in cancer chemotherapy and the drug delivery strategy outlined in this study also represents a promising approach for efficient delivery of hydrophilic drug molecules.

Acknowledgements

This work was financially supported by the Tianjin Research Program of Application Foundation and Advanced Technology (no. 13JCYBJC39300), Chinese Postdoctoral Science Foundation (2013M540062) and National Natural Science Foundation of China (81301309, 31300732). We would like to thank Professor Renjie Hu (Tianjin Institute of Medical and Pharmaceutical Science) for his collaboration of animal experiments.

References

1 X. Duan, J. Xiao, Q. Yin, Z. Zhang, H. Yu, S. Mao and Y. Li, *ACS Nano*, 2013, **7**, 5858–5869.
2 L. Bildstein, C. Dubernet and P. Couvreur, *Adv. Drug Delivery Rev.*, 2011, **63**, 3–23.
3 F. Greco and M. J. Vicent, *Adv. Drug Delivery Rev.*, 2009, **61**, 1203–1213.
4 J. A. Barreto, W. O'Malley, M. Kubeil, B. Graham, H. Stephan and L. Spiccia, *Adv. Mater.*, 2011, **23**, H18–H40.
5 R. Haag and F. Kratz, *Angew. Chem., Int. Ed.*, 2006, **45**, 1198–1215.
6 J.-H. Lee, K.-J. Chen, S.-H. Noh, M. A. Garcia, H. Wang, W.-Y. Lin, H. Jeong, B. J. Kong, D. B. Stout, J. Cheon and H.-R. Tseng, *Angew. Chem., Int. Ed.*, 2013, **52**, 4384–4388.
7 J. Liu, M. Yu, C. Zhou, S. Yang, X. Ning and J. Zheng, *J. Am. Chem. Soc.*, 2013, **135**, 4978–4981.
8 V. Torchilin, *Adv. Drug Delivery Rev.*, 2011, **63**, 131–135.

9 D. Chitkara, A. Mittal, S. W. Behrman, N. Kumar and R. I. Mahato, *Bioconjugate Chem.*, 2013, **24**, 1161–1173.
10 M. Dasari, A. P. Acharya, D. Kim, S. Lee, S. Lee, J. Rhea, R. Molinaro and N. Murthy, *Bioconjugate Chem.*, 2013, **24**, 4–8.
11 D. Trung Bui, A. Maksimenko, D. Desmaële, S. Harrisson, C. Vauthier, P. Couvreur and J. Nicolas, *Biomacromolecules*, 2013, **14**, 2837–2847.
12 S. Harrisson, J. Nicolas, A. Maksimenko, D. T. Bui, J. Mougin and P. Couvreur, *Angew. Chem., Int. Ed.*, 2013, **52**, 1678–1682.
13 D. Yang, X. Liu, X. Jiang, Y. Liu, W. Ying, H. Wang, H. Bai, W. D. Taylor, Y. Wang, J.-P. Clamme, E. Co, P. Chivukula, K. Y. Tsang, Y. Jin and L. Yu, *J. Controlled Release*, 2012, **161**, 124–131.
14 B. Jung, Y.-C. Jeong, J.-H. Min, J.-E. Kim, Y.-J. Song, J.-K. Park, J.-H. Park and J.-D. Kim, *J. Mater. Chem.*, 2012, **22**, 9385.
15 P. Gou, W. Liu, W. Mao, J. Tang, Y. Shen and M. Sui, *J. Mater. Chem. B*, 2013, **1**, 284.
16 H. Song, H. Xiao, Y. Zhang, H. Cai, R. Wang, Y. Zheng, Y. Huang, Y. Li, Z. Xie, T. Liu and X. Jing, *J. Mater. Chem. B*, 2013, **1**, 762–772.
17 S. Maiti, N. Park, J. H. Han, H. M. Jeon, J. H. Lee, S. Bhuniya, C. Kang and J. S. Kim, *J. Am. Chem. Soc.*, 2013, **135**, 4567–4572.
18 J. Rautio, H. Kumpulainen, T. Heimbach, R. Oliyai, D. Oh, T. Järvinen and J. Savolainen, *Nat. Rev. Drug Discovery*, 2008, **7**, 255–270.
19 D. Robinson and G. Keating, *Drugs*, 2006, **66**, 941–948.
20 W. J. Gradishar, *Expert Opin. Pharmacother.*, 2006, **7**, 1041–1053.
21 R. B. Greenwald, Y. H. Choe, J. McGuire and C. D. Conover, *Adv. Drug Delivery Rev.*, 2003, **55**, 217–250.
22 G. Pasut, F. Canal, L. D. Via, S. Arpicco, F. A. Veronese and O. Schiavon, *J. Controlled Release*, 2008, **127**, 239–248.
23 L. Seymour, *Int. J. Oncol.*, 2009, **34**, 1629–1636.
24 O. Soepenberg, M. J. A. de Jonge, A. Sparreboom, P. de Bruin, F. A. L. M. Eskens, G. de Heus, J. Wanders, P. Cheverton, M. P. Ducharme and J. Verweij, *Clin. Cancer Res.*, 2005, **11**, 1504–711.
25 H. Xiao, R. Qi, S. Liu, X. Hu, T. Duan, Y. Zheng, Y. Huang and X. Jing, *Biomaterials*, 2011, **32**, 7732–7739.
26 H. Xiao, H. Song, Q. Yang, H. Cai, R. Qi, L. Yan, S. Liu, Y. Zheng, Y. Huang, T. Liu and X. Jing, *Biomaterials*, 2012, **33**, 6507–6519.
27 H. Xiao, H. Song, Y. Zhang, R. Qi, R. Wang, Z. Xie, Y. Huang, Y. Li, Y. Wu and X. Jing, *Biomaterials*, 2012, **33**, 8657–8669.
28 D. Zhou, H. Xiao, F. Meng, S. Zhou, J. Guo, X. Li, X. Jing and Y. Huang, *Bioconjugate Chem.*, 2012, **23**, 2335–2343.
29 H. Xiao, L. Yan, Y. Zhang, R. Qi, W. Li, R. Wang, S. Liu, Y. Huang, Y. Li and X. Jing, *Chem. Commun.*, 2012, **48**, 10730–10732.
30 Y. Wang, H. Wang, Y. Chen, X. Liu, Q. Jin and J. Ji, *Chem. Commun.*, 2013, **49**, 7123–7125.
31 Z. Yuan, X. Yi, J. Zhang, S. Cheng, R. Zhuo and F. Li, *Chem. Commun.*, 2013, **49**, 801–803.
32 H. Wang, F. Xu, D. Li, X. Liu, Q. Jin and J. Ji, *Polym. Chem.*, 2013, **4**, 2004–2010.
33 S. Zhu, D. S. P. Lansakara-P, X. Li and Z. Cui, *Bioconjugate Chem.*, 2012, **23**, 966–980.
34 J. T. Lai, D. Filla and R. Shea, *Macromolecules*, 2002, **35**, 6754–6756.
35 E. Moysan, G. Bastiat and J.-P. Benoit, *Mol. Pharmaceutics*, 2013, **10**, 430–444.
36 M. Vandana and S. K. Sahoo, *Biomaterials*, 2010, **31**, 9340–9356.
37 A. Schmittel, R. Schuster, N. E. Bechrakis, J. M. Siehl, M. H. Foerster, E. Thiel and U. Keilholz, *Melanoma Res.*, 2005, **15**, 447–451.
38 A. Laromaine, L. Koh, M. Murugesan, R. Ulijn and M. Stevens, *J. Am. Chem. Soc.*, 2007, **129**, 4156–4157.
39 Y. Xu, Z. Liu, X. Zhang, Y. Wang, J. Tian, Y. Huang, Y. Ma, X. Zhang and Y. Chen, *Adv. Mater.*, 2009, **21**, 1275–1279.
40 J. Yao, L. Zhang, J. Zhou, H. Liu and Q. Zhang, *Mol. Pharmaceutics*, 2013, **10**, 1080–1091.
41 J.-K. Kim, M. D. Howard, T. D. Dziubla, J. J. Rinehart, M. Jay and X. Lu, *ACS Nano*, 2011, **5**, 209–216.
42 G. Bajaj, M. R. Kim, S. I. Mohammed and Y. Yeo, *J. Controlled Release*, 2012, **158**, 386–392.
43 C. Yang, A. Dantzig and C. Pidgeon, *Pharm. Res.*, 1999, **16**, 1331–1343.
44 P. M. Potter and R. M. Wadkins, *Curr. Med. Chem.*, 2006, **13**, 1045–1054.
45 P. Xu, E. A. Van Kirk, Y. Zhan, W. J. Murdoch, M. Radosz and Y. Shen, *Angew. Chem., Int. Ed.*, 2007, **46**, 4999–5002.
46 C. Li, *Adv. Drug Delivery Rev.*, 2002, **54**, 695–713.
47 V. Alt, T. Bechert, P. Steinrücke, M. Wagener, P. Seidel, E. Dingeldein, E. Domann and R. Schnettler, *Biomaterials*, 2004, **25**, 4383–4391.
48 S. M. Horowitz, C. G. Frondoza and D. W. Lennox, *J. Orthop. Res.*, 1988, **6**, 827–832.
49 Y.-Q. Wang, Y.-X. Sun, X.-L. Hong, X.-Z. Zhang and G.-Y. Zhang, *Mol. BioSyst.*, 2010, **6**, 256–263.
50 Y. Min, C.-Q. Mao, S. Chen, G. Ma, J. Wang and Y. Liu, *Angew. Chem., Int. Ed.*, 2012, **51**, 6742–6747.
51 J.-Z. Du, X.-J. Du, C.-Q. Mao and J. Wang, *J. Am. Chem. Soc.*, 2011, **133**, 17560–17563.
52 T. Hoang, K. Kim, A. Jaslowski, P. Koch, P. Beatty, J. McGovern, M. Quisumbing, G. Shapiro, R. Witte and J. H. Schiller, *J. Lung Cancer*, 2003, **42**, 97–102.
53 L. H. Reddy, J.-M. Renoir, V. Marsaud, S. Lepetre-Mouelhi, D. Desmaële and P. Couvreur, *Mol. Pharmaceutics*, 2009, **6**, 1526–1535.
54 S. Dufort, L. Sancey and J.-L. Coll, *Adv. Drug Delivery Rev.*, 2012, **64**, 179–189.